

Use of the Global Positioning System for Evaluating Inertial Measurement Unit Errors

John J. Dougherty, Hossny El-Sherief, and David S. Hohman
TRW Systems Integration Group, San Bernardino, California 92402

A trajectory reference system based on the Global Positioning System (GPS) can be used instead of conventional radars during missile flight tests. The high quality of the GPS-based trajectory reference makes it useful for evaluating the performance of the missiles' inertial measurement units. Such a system was installed and flight tested on two recently launched ballistic missiles. The GPS hardware configuration used on these flights is described. A Kalman filter approach is used to estimate individual inertial measurement unit errors based on the GPS range and delta range data. The ability of the GPS-based system to identify inertial measurement unit errors is compared to that of radar; the GPS is found to provide superior estimates.

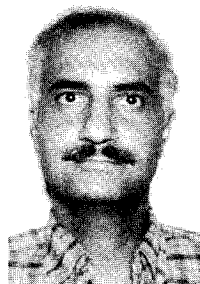
Introduction

THE Global Positioning System (GPS) is a satellite navigation system under development by the United States Department of Defense. In its final configuration it will consist of 24 satellites in semigeosynchronous orbit providing continuous global coverage and excellent navigation accuracy.¹⁻³

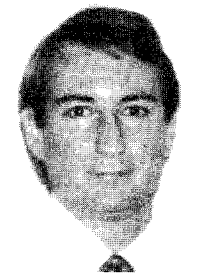
Because of the versatility provided by the global availability and the passive nature of the user segment, the GPS is being used in a wide range of applications.^{4,5} One of these is as a trajectory reference for missile flight testing; specifically, the GPS is being used to evaluate the errors in a missile's inertial measurement unit (IMU).⁶



John J. Dougherty received a Bachelor of Mechanical Engineering degree from the University of Dayton in 1984 and a M.S. degree in Aeronautical and Astronautical Engineering from Stanford University in 1985. He is currently a Ph.D. candidate at the University of California at Los Angeles in the field of trajectory optimization. From 1986 to the present he has worked at the Guidance, Systems, and Controls Department at TRW. Prior to that he worked at the Air Force Wright Aeronautical Laboratories Compressor Research Facility and McDonnell Aircraft's Flight Simulation department. His interests include inertial navigation, system simulation, and test data analysis.



Hossny El-Sherief was born in Egypt, in 1950. He received BS in Mathematics from AinShams University and BS from Cairo University, MS and PhD from McMaster University; all in Electrical Engineering. Joined TRW in 1987 and is currently senior manager, Guidance, Systems and Controls Department. Joined Exxon Research in 1981 as engineering specialist developing seismic signal processing techniques. Taught Controls, Signal Processing, and Estimation at McMaster University and University of Petroleum and Minerals. He is member of the Electrical Engineering Advisory Board, California State University, Long Beach and University of Nevada, Reno. He published over 40 papers in the areas of estimation, control, guidance and GPS.



David S. Hohman received his B.S. degree in 1985 and his M.S. degree in 1987, both in electrical engineering from the University of Delaware. He is a Senior Professional Staff member at the Johns Hopkins University, Applied Physics Laboratory, Strategic Systems Department. The last four years, Mr. Hohman has worked on evaluating the performance of missile guidance and navigation systems at TRW. His other interests include digital signal/image processing, pattern recognition, adaptive filtering and neural network implementation.

Received Dec. 15, 1992; revision received Aug. 5, 1993; accepted for publication Aug. 5, 1993. Copyright © 1993 by the American Institute of Aeronautics and Astronautics, Inc. All rights reserved.

This paper was presented at the AIAA Guidance, Navigation, and Control Conference at Monterey, CA, 9-11 August 1993, paper #AIAA-93-3887-CP, proceedings Vol. 3, pp. 1678-1685.

Flight testing is used in both the development and the operational evaluation of intercontinental ballistic missiles (ICBMs) for the purpose of assessing system function and impact accuracy. In an ICBM system, the missile deploys one or more re-entry vehicles, which fall ballistically to a target. A major goal of ICBM design is to minimize re-entry vehicle miss, the distance between the re-entry vehicle's actual impact point and the target point. An important contributor to this miss is error in the information produced by the IMU; a corresponding goal of flight testing is to quantify the magnitude of this error and its effect on impact accuracy.

Isolating the contribution to miss from the IMU and estimating the sources of the IMU error require a separate trajectory reference. In the past, ground-based radars and, sometimes, a second onboard IMU have been used to provide the reference. The second option is usually prohibitive in terms of both cost and payload restrictions, while radars suffer from limitations in both geometry and accuracy. Recent United States Air Force (USAF) flight testing has demonstrated that the GPS can provide a small, light, affordable, and accurate trajectory reference system for flight testing ICBMs. Some of the technology used had been demonstrated previously by the United States Navy during Trident I (Ref. 7) and Trident II (Ref. 8) missile testing.

For several years the United States Navy has used a GPS-based measurement system to evaluate IMU errors during their Trident submarine-launched ballistic missile flight testing. The Navy's experience indicated that the GPS would provide a trajectory reference superior to that from radar, allowing for higher confidence estimates of IMU errors. To demonstrate the usefulness of the GPS for evaluating IMU errors on a USAF ICBM, two operational Peacekeeper missiles were outfitted with GPS translators and triband antennas prior to being launched from Vandenberg Air Force Base in California to the Kwajalein Atoll target area in the Pacific Ocean.

The following paper describes the GPS flight testing, the data analysis techniques, the results, and conclusions. The hardware used during the flight testing represented a new approach to two-channel translation of GPS signals; it is described in the next section.

A Kalman filter has been used for many years in evaluating IMU errors using radar data. A similar approach to evaluating IMU errors using GPS data was employed here, with some differences. Results from the flight tests are presented. Various measures of performance indicate that GPS data allowed for higher confidence estimates, as compared to those from radar, of the contribution of the IMU errors to miss. Following the results are conclusions.

Global Positioning System Hardware Configuration

The two Peacekeeper missiles used to demonstrate the usefulness of the GPS for IMU evaluations, designated GT-06 and GT-07, carried dual-frequency GPS translators and triband antennas. Unlike a GPS receiver, which generates trajectory information from the received GPS signals, a translator merely retransmits the GPS data on a different carrier frequency. Translators rather than receivers were used because of their low cost, weight, and power consumption, and because translated GPS signals allowed for extensive corrections to be applied to the GPS data after the flight. The triband antenna allowed for reception of L-band GPS signals and the retransmission of the GPS signals on S-band. The S-band is also used by the missile telemetry system. In addition, the missile carried a C-band transponder to aid in radar tracking.

The Peacekeeper GPS experiment used CA-code from the L_1 (1575 MHz) frequency and P-code from the L_2 (1227 MHz) frequency. To reduce translator power consumption, the 20 MHz L_2 P-code signal was crammed into a 2 MHz bandwidth during translation, causing some loss of resolution. The L_1 signal was used directly to generate range and phase-derived delta range missile tracking data, while the L_2 signal was used to

correct for atmospheric refraction. The feasibility of cramming the L_2 signal for this purpose had not been demonstrated before. Without useful L_2 data, cruder corrections based on empirical models would have been used instead.

For each flight, useful data from six satellites were available throughout powered flight. The translated GPS signals were recorded at ground receiving stations located at Vandenberg Air Force Base and at Pillar Point, near San Francisco.

Inertial Measurement Unit Evaluation Method

The goals of an IMU evaluation are to determine the total miss due to the IMU, to determine the contribution due to each of the major IMU error groups, such as total accelerometer, total gyro, IMU clock, and initial conditions, and to determine (as best as possible) the identities of the largest of the individual contributors, such as individual instrument biases and scale factors. Given telemetered IMU data and range instrumentation data (GPS or radar) from a missile flight test, a Kalman filter can be used to form an estimate of the magnitude of the IMU calibration, instrument drift, and initial condition (including alignment) errors. Estimates of the contributions to miss of these individual errors, as well as group and IMU totals, can then be calculated.

The general approach to evaluating IMU errors is to process IMU telemetry data together with the range instrumentation data to generate measurements that are a function of the IMU errors and the range instrumentation errors. Error models for accelerometers, gyros, the IMU clock, and initial conditions are combined with differential equations for the propagation of errors in an inertial navigation system to produce the sensitivities of these measurements to IMU errors. Likewise, error models for the range instrumentation system are used to generate the sensitivities of the measurements to GPS or radar errors. The measurements and error sensitivities are used in a Kalman filter to generate estimates of the error magnitudes for the flight, which in turn can be used to calculate the effects of the IMU error magnitudes on impact miss. A flowchart for a typical IMU evaluation using the GPS is shown in Fig. 1; an evaluation using radar data is similar.

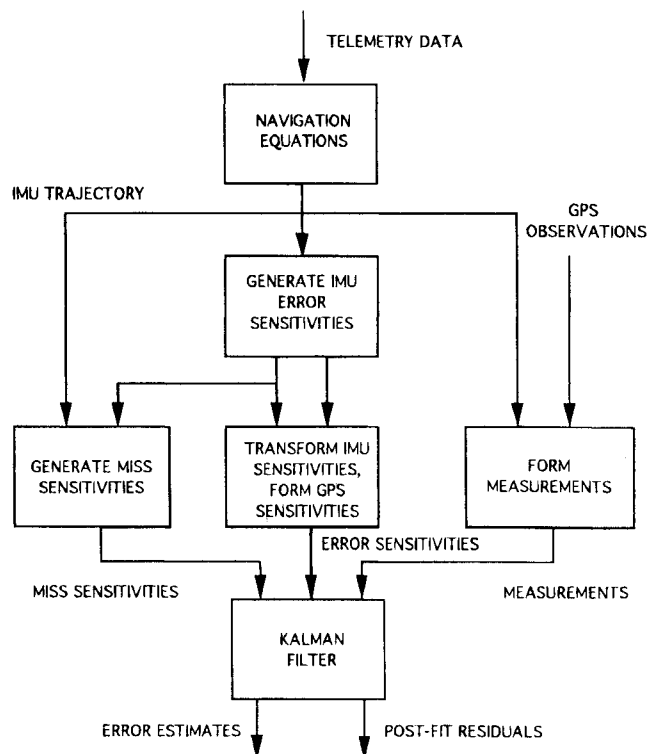


Fig. 1 Postflight IMU evaluation.

Measurements

The first step in estimating IMU errors is to form an ideal navigated trajectory. This trajectory is produced by processing raw accelerometer data, obtained from telemetry, through accurate navigation equations on a high-precision computer using best estimates of initial conditions and Department of Defense WGS-84 8×8 gravity, including launch-region gravity.⁹ Any error in this trajectory results, by definition, from IMU errors, and therefore the trajectory is called the IMU-indicated trajectory.¹⁰

Once an IMU-indicated trajectory is formed, it is transformed to the range instrumentation domain (range and delta range for GPS, range and range rate for radar), synchronized, and differenced with the range instrumentation measurement. The differences are nonzero due to IMU errors, modeled and unmodeled range instrumentation errors, and random noise.

For the GPS, the measurement system data represent the satellite-to-missile-to-receiver (ground) path length, for range, or the change of that path length over some time interval, for delta range. These data are edited and corrected for ionospheric, tropospheric, and antenna lever-arm effects, known clock and timing errors, relativity, and other effects.¹¹ The differences between these measurements and the equivalent IMU-indicated quantity are known as single-link range and delta range (or doppler) measurements. To eliminate common missile-to-receiver downlink errors, the single-link measurements are differenced by pairs.⁸ The results are used as Kalman filter measurements.

Specifically, for range, the GPS data arrive as

$$R_{\text{GPS}}^i(t_k) = r^i(t_k) + M_{R/\text{GPS}}^i(t_k) x_{\text{GPS}}(t_k) + \rho(t_k) + e_{\text{GPS}}(t_k) + v_R^i(t_k) \quad (1)$$

where R_{GPS}^i is the GPS-measured satellite-to-missile-to-ground range for the i th link, r^i is the true satellite-to-missile range, $M_{R/\text{GPS}}^i$ is the sensitivity to GPS error sources of satellite-to-missile range, x_{GPS} is a vector of the GPS error sources, ρ is the true missile-to-ground range, e_{GPS} is the GPS downlink error common to all satellites, and v_R^i is the GPS range measurement noise.

The equivalent IMU-indicated quantity is

$$R_{\text{IMU}}^i(t_k) = r^i(t_k) + M_{R/\text{IMU}}^i(t_k) x_{\text{IMU}}(t_k) + \rho(t_k) + e_{\text{IMU}}(t_k) \quad (2)$$

where R_{IMU}^i is the IMU-indicated satellite-to-missile-to-ground range for the i th link, $M_{R/\text{IMU}}^i$ is the sensitivity to IMU error sources of satellite to missile range, x_{IMU} is a vector of the IMU error sources, and e_{IMU} is the IMU error in the indication of the missile-to-ground range.

The single-link range measurements for the i th link are then

$$\begin{aligned} R_{\text{GPS}}^i(t_k) - R_{\text{IMU}}^i(t_k) &= M_{R/\text{GPS}}^i(t_k) x_{\text{GPS}}(t_k) \\ &+ e_{\text{GPS}}(t_k) + v_R^i(t_k) - [M_{R/\text{IMU}}^i(t_k) x_{\text{IMU}}(t_k) + e_{\text{IMU}}(t_k)] \\ &= M_R^i(t_k) x(t_k) + v_R^i(t_k) + e_{\text{GPS}}(t_k) - e_{\text{IMU}}(t_k) \end{aligned}$$

where M_R^i and x are defined appropriately.

The Kalman filter measurements are formed by differencing the single-link measurements for the i th and j th links:

$$\begin{aligned} z_R^{ij}(t_k) &= [R_{\text{GPS}}^i(t_k) - R_{\text{IMU}}^i(t_k)] - [R_{\text{GPS}}^j(t_k) - R_{\text{IMU}}^j(t_k)] \\ &= M_R^i(t_k) x(t_k) + v_R^i(t_k) - [M_R^j(t_k) x(t_k) + v_R^j(t_k)] \quad (4) \\ &= [M_R^i(t_k) - M_R^j(t_k)] x(t_k) + [v_R^i(t_k) - v_R^j(t_k)] \end{aligned}$$

Thus, the filter measurements are functions only of the IMU and GPS errors and noise, and are free of the relatively large GPS downlink errors.

The same is done for the GPS delta range measurement:

$$\begin{aligned} D_{\text{GPS}}^i(t_k) &= r^i(t_k) + M_{D/\text{GPS}}^i(t_k) x_{\text{GPS}}(t_k) + \rho(t_k) + e_{\text{GPS}}(t_k) \\ &+ v_{\text{AC}}^i(t_k) - [r^i(t_{k-1}) + M_{D/\text{GPS}}^i(t_{k-1}) x_{\text{GPS}}(t_{k-1}) \\ &+ \rho(t_{k-1}) + e_{\text{GPS}}(t_{k-1}) + v_{\text{AC}}^i(t_{k-1})] + v_D^i(t_k) \end{aligned} \quad (5)$$

where $D_{\text{GPS}}^i(t_k)$ is the GPS-measured satellite-to-missile-to-ground delta range for the i th link from time t_{k-1} to time t_k , $M_{D/\text{GPS}}^i$ is the sensitivity to GPS error sources of satellite-to-missile, phase-derived range, v_{AC}^i is the GPS phase-derived range one-step anticorrelated measurement noise, and v_D^i is the GPS phase-derived delta range measurement noise.

The equivalent IMU-indicated quantity is

$$\begin{aligned} D_{\text{IMU}}^i(t_k) &= r^i(t_k) + M_{D/\text{IMU}}^i(t_k) x_{\text{IMU}}(t_k) + \rho(t_k) \\ &+ e_{\text{IMU}}(t_k) x_{\text{IMU}}(t_k) - [r^i(t_{k-1}) + M_{D/\text{IMU}}^i(t_{k-1}) x_{\text{IMU}}(t_{k-1}) \\ &+ \rho(t_{k-1}) + e_{\text{IMU}}(t_{k-1})] \end{aligned} \quad (6)$$

The single link delta range measurements for the i th link are then

$$\begin{aligned} D_{\text{GPS}}^i(t_k) - D_{\text{IMU}}^i(t_k) &= M_{D/\text{GPS}}^i(t_k) x_{\text{GPS}}(t_k) + e_{\text{GPS}}(t_k) + v_{\text{AC}}^i(t_k) \\ &- [M_{D/\text{GPS}}^i(t_{k-1}) x_{\text{GPS}}(t_{k-1}) + e_{\text{GPS}}(t_{k-1}) + v_{\text{AC}}^i(t_{k-1})] \\ &+ v_D^i(t_k) \\ &- \{M_{D/\text{IMU}}^i(t_k) x_{\text{IMU}}(t_k) + e_{\text{IMU}}(t_k) \\ &- [M_{D/\text{IMU}}^i(t_{k-1}) x_{\text{IMU}}(t_{k-1}) + e_{\text{IMU}}(t_{k-1})]\} \\ &= M_D^i(t_k) x(t_k) - M_D^i(t_{k-1}) x(t_{k-1}) + v_{\text{AC}}^i(t_k) \\ &- v_{\text{AC}}^i(t_{k-1}) + v_D^i(t_k) + e_{\text{GPS}}(t_k) - e_{\text{GPS}}(t_{k-1}) \\ &- [e_{\text{IMU}}(t_k) - e_{\text{IMU}}(t_{k-1})] \end{aligned} \quad (7)$$

where M_D^i is defined appropriately.

The Kalman filter measurements are formed by differencing the single-link measurements for the i th and j th links:

$$\begin{aligned} z_D^{ij}(t_k) &= [D_{\text{GPS}}^i(t_k) - D_{\text{IMU}}^i(t_k)] - [D_{\text{GPS}}^j(t_k) - D_{\text{IMU}}^j(t_k)] \\ &= M_D^i(t_k) x(t_k) - M_D^i(t_{k-1}) x(t_{k-1}) \\ &+ v_{\text{AC}}^i(t_k) - v_{\text{AC}}^i(t_{k-1}) + v_D^i(t_k) \\ &- [M_D^j(t_k) x(t_k) - M_D^j(t_{k-1}) x(t_{k-1}) \\ &+ v_{\text{AC}}^j(t_k) - v_{\text{AC}}^j(t_{k-1}) + v_D^j(t_k)] \end{aligned} \quad (8)$$

Again, the filter measurements are functions only of the IMU and GPS errors and noise, and are free of the relatively large GPS downlink errors.⁸

Typical plots (from flight GT-07) of single-link measurements for range and delta range are shown in Figs. 2 and 4.

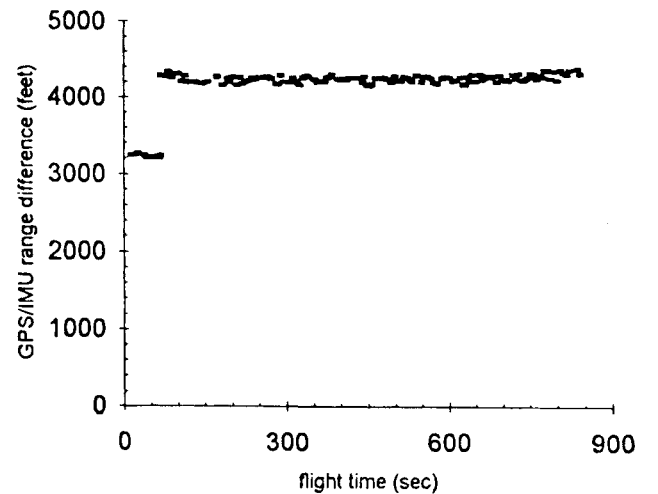


Fig. 2 Satellite NS 08 GPS minus IMU range.

These plots represent the difference between the IMU-indicated trajectory and each GPS measurement for a single satellite. Figures 3 and 5 contain differences in each of these quantities between two different satellites. Note that the common missile-to-receiver downlink errors evident in the single-link measurements are large compared to their differences, that is, the Kal-

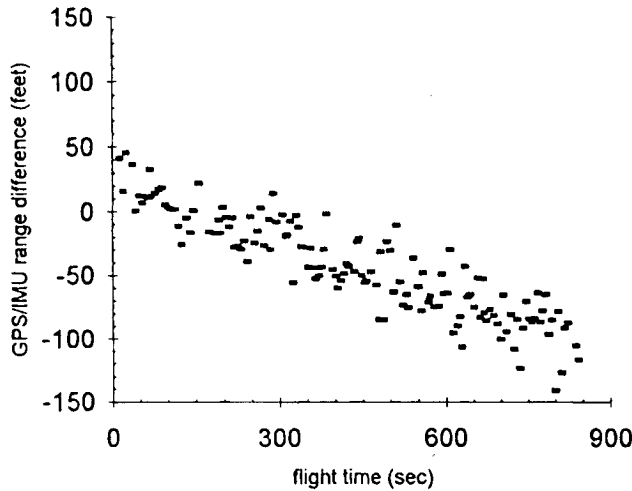


Fig. 3 Satellites NS 08 and 13 GPS minus IMU range differences.

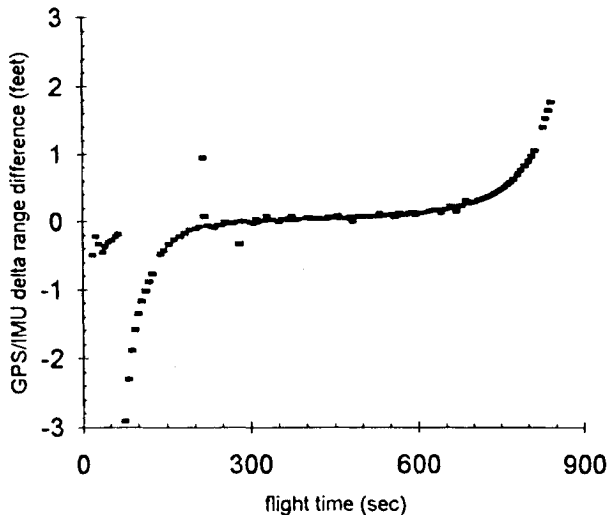


Fig. 4 Satellite NS 08 GPS minus IMU delta range.

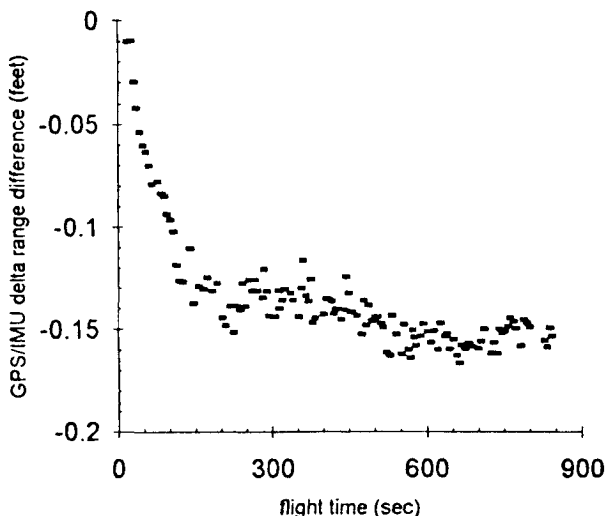


Fig. 5 Satellites NS 08 and 13 GPS minus IMU delta range differences.

man filter measurements, in Figs. 3 and 5. In particular, the large discontinuity occurring at about 61 s and visible in both the single-link range and delta range plots is removed by this technique. The first staging event occurred at about this time, and the plume impinging on the departing stage disrupted the missile-to-ground downlink common to translated signals from all satellites.

Error Models

The IMU error model used in an IMU evaluation can be varied, but in general consists of terms to account for errors in the accelerometers, gyros, IMU clock, and initial conditions. A successful technique that had been used in the past for radar analyses of the IMU had been to pick 12–15 of the most significant terms from a larger IMU model. A separate study conducted using actual flight test data confirmed that more terms are necessary when using GPS data, due to the increased quality of the GPS measurements over those from radar. Thus, a total of 73 terms were used, including 33 accelerometer terms, 30 gyro terms, one clock term, and nine initial condition terms. The same IMU terms were used for both the GPS and radar analyses so that the results could be more easily compared.

The IMU errors are modeled as being initially random but constant throughout the flight. Of course, the effects of the errors on the navigated state and the GPS or radar measurements are functions of time:

$$x_{\text{IMU}}(t_{k+1}) = x_{\text{IMU}}(t_k) \quad (9)$$

$$M_{R/\text{IMU}}^i(t_k) = \partial R^i(t_k) / \partial x_{\text{IMU}} \quad (10)$$

The typical GPS error model includes 12 terms for each satellite, five global terms, and random measurement noise. The errors include satellite position, velocity, and clock errors, tropospheric scale factor errors, antenna doppler errors, systematic range and delta range errors, lever-arm errors, and relative timing errors. Some of the errors are modeled as random constants (or biases):

$$x_{\text{GPS/BIAS}}(t_{k+1}) = x_{\text{GPS/BIAS}}(t_k) \quad (11)$$

Others are modeled as exponentially correlated random variables (a Gauss-Markov process):

$$x_{\text{GPS/MRKV}}(t_{k+1}) = \exp[-\beta(t_{k+1} - t_k)] x_{\text{GPS/MRKV}}(t_k) + w(t_k) \quad (12)$$

where

$$E[w(t_k)^2] = \sigma^2 * \{1 - \exp[-2\beta(t_{k+1} - t_k)]\} \quad (13)$$

For both bias and Markov errors, the effects of the errors on GPS measurements are functions of time:

$$M_{R/\text{GPS}}^i(t_k) = \partial R^i(t_k) / \partial x_{\text{GPS}} \quad (14)$$

$$M_{D/\text{GPS}}^i(t_k) = \partial D^i(t_k) / \partial x_{\text{GPS}} \quad (15)$$

The measurement noise for range, v_b^i , is modeled as white Gaussian noise. For the delta range, both v_b^i and v_{AC}^i are modeled as white Gaussian noise, although the actual delta range measurement is anticorrelated to the past value of v_{AC}^i , as seen in Eq. (5).¹²

The typical radar error model, used for many years in ICBM testing, has terms for range bias errors, range rate bias errors, radar site survey errors, relative timing errors, and random measurement noise. The errors are usually modeled as random constants, although the range bias error can be modeled as a random walk process. Angle data are generally not used in the analysis because of their relatively large noise content.

Kalman Filter

Measurement noise covariances, transition matrix elements, process noise covariance elements, and initial error state covariance matrices are generated prior to filtering the measurement data.

In the filter, the measurements are compared with the unit error sensitivities to form estimates of the IMU and range instrumentation error magnitudes.¹³ The Kalman state vector consists of a series of scalar error sources derived from models of the IMU and GPS or radar. The measurement vector consists of the differences between the IMU- and GPS- or radar-indicated trajectories, as described earlier.

The state-to-measurement transformation matrix, or simply the measurement matrix, consists of partial derivatives of the error model equations transformed to the GPS or radar measurement frames. The measurement matrix is a function of time. If the GPS is being used as the range instrumentation, the IMU error partial derivatives are transformed to range and delta range coordinates for each satellite link, resulting in the sensitivities of range and delta range measurements to unit IMU errors. These sensitivities are differenced by pairs across links to correspond to the GPS Kalman filter measurements. Sensitivities of the Kalman filter measurements to unit GPS error sources are also calculated. A similar procedure is used for radar.

Because errors in one satellite or radar do not affect measurements by another, the measurement matrix contains large blocks of zeros; this feature is exploited in the implementation of the equations to reduce the number of computations.

On the other hand, matters are complicated by the fact that data from the various GPS satellites are not uniformly available. Likewise, radars tend to acquire, lose, and reacquire track at different times throughout the flight. Since the number of satellites or radars for which there are observations available varies, the total number of measurements is time dependent. This situation is handled by adjusting the size and composition of the measurement vectors and the covariance and measurement matrices so as to include only those measurements corresponding to active satellites or radars.

Once the filter has arrived at estimates of the IMU error magnitudes, they are propagated into impact space using the error sensitivities at deployment and precalculated miss coefficients.

Flight Test Results

The Peacekeeper GPS hardware performed as designed on flight tests GT-06 and GT-07. The L_1 CA-code was used to obtain range data and phase-derived delta range data. The L_2 crammed P-code signal was recovered, allowing for good corrections for atmospheric refraction.

Evaluations of the performance of the IMU on both GT-06 and GT-07 were conducted using, in turn, GPS and radar data. The error estimates, especially those derived from the GPS data, provided good insight into the performance of the IMU. The question of the relative performance of the two instrumentation systems is addressed by considering various measures of confidence in the estimates.

The filters ability to identify IMU error magnitudes depends in part on the geometry of the range instrumentation system. A common measure of this geometry is the position dilution of precision (PDOP). A desired GPS PDOP of 3.5 or less had been used as one of the preflight planning criteria to ensure good data for the IMU evaluation. Plots of PDOP for GPS and radar for GT-07 are presented in Figs. 6 and 7. The six GPS satellites provided excellent geometry throughout the flight. On the other hand, the PDOP for radar indicates poor geometry for a significant portion of the flight. A typical array of radars was used for these flights, with six to eight radars along the coast of California and one or two more in Hawaii. The PDOP for radar was infinite until the missile broke horizon at enough California sites; it then degraded dramatically as the missile

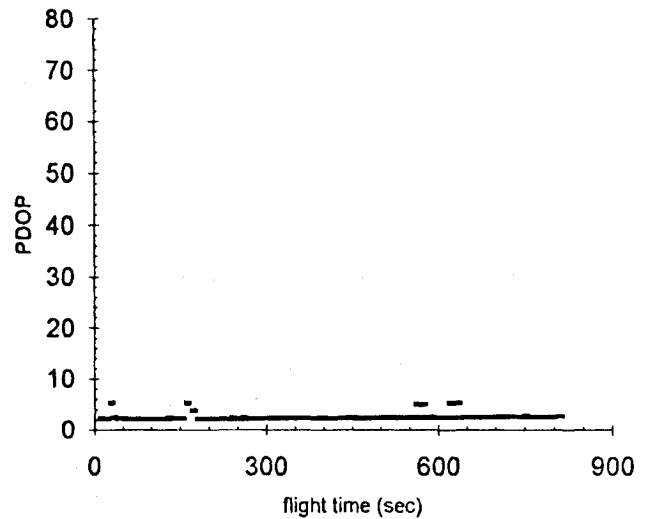


Fig. 6 GT-07 PDOP using GPS.

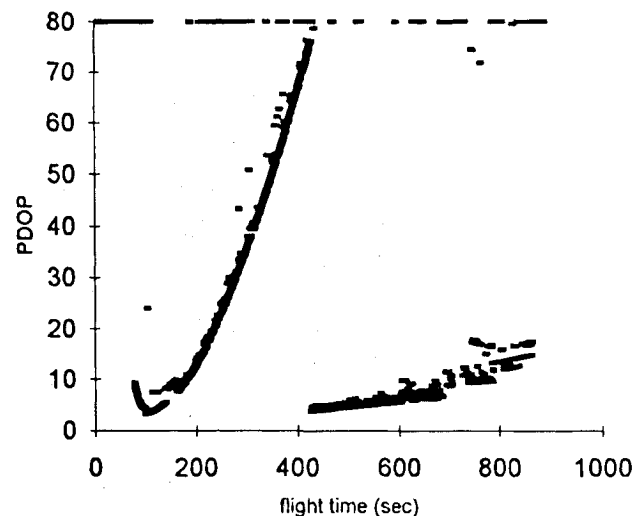


Fig. 7 GT-07 PDOP using radar.

Table 1 GT-07 GPS and radar relative estimation uncertainties

	GPS		Radar	
	DR ^a	CR	DR	CR
Initial conditions	0.64	0.64	0.81	1.24
Accelerometers	0.94	0.34	0.98	0.34
Gyros	0.09	0.56	0.13	1.28
Clock	0.56	0.01	0.73	0.81
Total	0.26	0.03	0.64	0.77

^aDownrange (DR) and crossrange (CR) uncertainties normalized by the total radial uncertainty for radar.

departed the mainland. Acquisition by the midrange (Hawaii) radars provided a marked improvement.

An indication of the filter's performance is the magnitude of the a posteriori or estimation uncertainties. Table 1 shows impact space (downrange and crossrange) estimation uncertainties for GT-07 GPS and radar. The uncertainties are normalized by the total radial uncertainty for radar. These are idealized uncertainties; engineering uncertainties would be somewhat higher because the a priori uncertainties are estimates themselves and because of the error models are only an approximate description of the actual physics. Nevertheless, the estimation uncertainties still provide a relative scale for comparing the GPS and radar. The GPS had lower (better) uncertainties on

the estimates of total miss due to the IMU. The GPS also had lower uncertainties on the estimates of the miss due to the major IMU error groups.

Note that both systems had lower uncertainties on the estimate of total miss than on the estimates of the group misses because of the high correlation between estimates of the individual states. In other words, the estimation error for the various individual states was correlated, and therefore the estimation error for one group of states was correlated to the estimation error for other groups of states. Physically, this means that the instrumentation systems (both GPS and radar) allow for a good estimate of the missile trajectory and, in particular, the deployment state, but they do not do as well in discerning the subtle differences in the ways individual errors propagate. The result is an inability to estimate the contribution of any group of errors with as much confidence as the total. This limitation of flight testing IMUs on ICBMs has been confirmed by simulation.¹⁴

Another measure of the ability of the filter to estimate IMU errors is the error recovery ratio. The recovery ratio for an error is the ratio of the square root of the corresponding diagonal element of the final error covariance matrix divided by the square root of the same diagonal element of the initial covariance matrix. It represents the ratio of final uncertainty to initial uncertainty for an individual error; low recovery ratios indicate better estimates. Recovery ratios do not include any of the correlation information in the final error covariance matrix. For this problem, the initial covariances were established based on preflight tests (for the IMU) or previous system performance (for GPS or radar) and were not altered during the postflight analysis. Therefore, the recovery ratios are indicative of the final uncertainty and provide a common measure for comparing GPS and radar performance.

A similar measure of estimation uncertainty, defined for groups of errors, is termed the grouped error recovery ratio. It is defined as the ratio of the circular error probable (CEP) derived from the final impact-space covariance matrix for the group divided by the CEP derived from the corresponding initial impact-space covariance matrix. The impact-space covariance matrices are calculated from state-space submatrices, consisting of rows and columns of the error covariance matrix corresponding to the individual errors belonging to the group in question, propagated into impact space. This measure is related to, but not the same as, the grouped uncertainties presented in Table 1. Of course, one group of errors is the set of all IMU errors, referred to as the total IMU error.

Figure 8 shows the grouped and total error recovery ratios for the GPS and radar for GT-07. Again, the GPS did a better job than radar of estimating grouped and total IMU errors; both the GPS and radar estimated the total better than the groups.

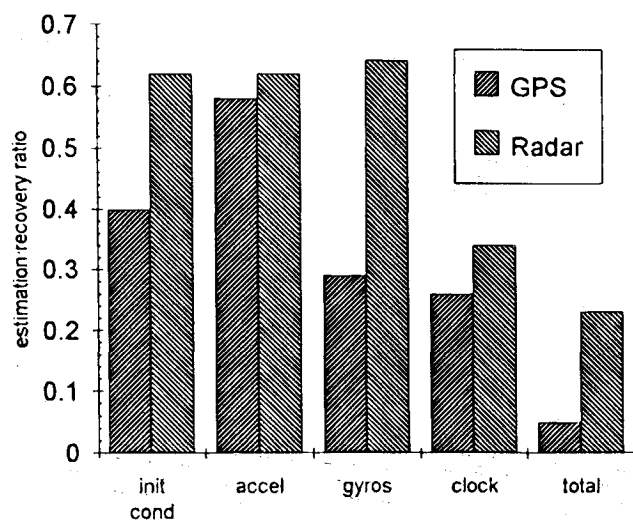


Fig. 8 GPS and radar grouped error recovery.

Figure 9 shows the distribution of individual error recovery ratios. The GPS was able to estimate 25 terms and radar was able to estimate nine terms with a recovery ratio of 0.9 or less. Thus, while both systems were limited in their ability to discern the effects of individual terms in a large IMU model, the capability of the GPS significantly exceeded that of radar.

An unexpected result of the IMU evaluation using the GPS was the confirmation of a launch site survey error. This error was not apparent in the radar results.

Summary of Flight Test Results

Estimates of the total miss due to the IMU errors, the miss due to major groups of IMU errors, and the miss due to individual IMU errors were obtained using the GPS and radar.

Various measures of Kalman filter performance and error observability, such as PDOP, the total estimation uncertainties, and the total error recovery ratios, indicate that the GPS produced higher confidence estimates of the total miss due to IMU errors than radar.

Measures such as PDOP, grouped estimation uncertainties, and the grouped error recovery ratios indicate that the GPS did a better job of estimating the miss due to major groups of IMU errors than radar. For both the GPS and radar, however, the confidence in the group estimates is lower than the confidence in the estimates of total miss due to IMU errors.

Measures such as PDOP and the individual error recovery ratios indicate that the GPS did a better job of estimating the miss due to individual IMU errors than radar. Specifically, the GPS had better visibility into more error terms than radar. For both the GPS and radar, however, the confidence in most individual error estimates is low. Thus, while the total miss due to the IMU is well-known, the miss estimates for individual errors are highly correlated and the miss due to any single error source is not well-known.

Conclusions

The Peacekeeper GPS test flights were extremely successful. All flight hardware, postflight tracking hardware and software, and postflight inertial measurement unit evaluation software performed as designed. The GPS proved to be a valuable tool for assessing inertial measurement unit errors during the flight tests. It provided excellent geometry and low noise data, which allowed for estimates of inertial measurement unit errors superior to those obtained with radar.

Acknowledgment

This work has been performed in support of the United States Air Force Development Support Organization, Norton Air Force Base, California, under contract number F04704-92-C-0005.

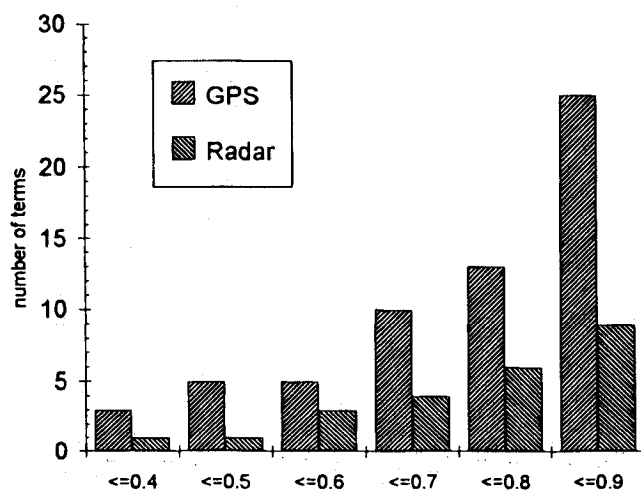


Fig. 9 GPS and radar individual error recovery.

References

- ¹ Milliken, R. J., and Zoller, C. J., "Principle of Operation of NAVSTAR and System Characteristics," *Global Positioning System Papers*, edited by P. Janiczek and S. Gilbert, Vol. I, Inst. of Navigation, Washington, DC, 1980, pp. 3-14.
- ² Spilker, J. J., Jr., "GPS Signal Structure and Performance Characteristics," *Global Positioning System Papers*, edited by P. Janiczek and S. Gilbert, Vol. I, Inst. of Navigation, Washington, DC, 1980, pp. 29-54.
- ³ Anon., "NAVSTAR GPS User Equipment" (Public Release Version), U.S. Air Force Space Systems Div., NAVSTAR-GPS Joint Program Office, Los Angeles, CA, Feb. 1991.
- ⁴ Kao, M. H., and Eller, D. H., "Multiconfiguration Kalman Filter Design for High-Performance GPS Navigation," *IEEE Transactions on Automatic Control*, Vol. AC-28, No. 3, 1983, pp. 304-314.
- ⁵ Simon, D. J., and El-Sherief, H., "Design of Global Positioning System Receivers for Integrated Inertial Navigation Systems," *Proceedings of the 32nd IEEE Conference on Decision and Control*, San Antonio, TX, Inst. of Electrical and Electronics Engineers, Piscataway, NJ, 1993, pp. 1476-1477.
- ⁶ Dougherty, J. J., El-Sherief, H., Simon, D. J., and Whitmer, G. A., "A Design Approach for a GPS User Segment for Aerospace Vehicles," *Proceedings of the American Control Conference*, San Francisco, CA, Inst. of Electrical and Electronics Engineers, Piscataway, NJ, 1993, pp. 935-939.
- ⁷ Levy, L., "SATRACK Development," *Johns Hopkins University Applied Physics Laboratory Developments in Science and Technology*, Vol. 6, Johns Hopkins Univ. Applied Physics Lab., Laurel, MD, 1978, pp. 98-100.
- ⁸ Vetter, J. R., Schwenk, V. L., and Hattox, T. M., "An Improved GPS Based Tracking System for High Accuracy Trident II Missile Navigation and Guidance Evaluation," *Proceedings of the Fourteenth Biennial Guidance Test Symposium*, Vol. II, 6585th Test Group, Holloman Air Force Base, NM, 1989, pp. 67-86.
- ⁹ Anon., "Dept. of Defense World Geodetic System 1984," DMA TR 8350.2, Defense Mapping Agency, Washington, DC, Sept. 30, 1987.
- ¹⁰ Anon., "Post Flight Data Analysis and Handling Plan for Peacekeeper Missile Guidance and Control System Performance and Accuracy Assessment," C82-853/201, Rockwell International, Anaheim, CA, Oct. 14, 1983.
- ¹¹ Anon., "GPS Preprocessing and Data Validation," Johns Hopkins Univ. Applied Physics Lab., Jan. 10, 1990.
- ¹² Anon., "GPS Peacekeeper Demonstration Flight Test Program Modeling Handbook," Charles Stark Draper Lab., Cambridge, MA, revised Sept. 1991, pp. H1-H23.
- ¹³ Anon., *Applied Optimal Estimation*, edited by Arthur Gelb, Massachusetts Inst. of Technology Press, Cambridge, MA, 1974, ch. 4.
- ¹⁴ Dougherty, J. J., El-Sherief, H., and Simon, D. J., "Application of GPS for Missile Post Flight Guidance Accuracy Analysis," *Proceedings of the First IEEE Regional Conference on Aerospace Control Systems*, Westlake Village, CA, Inst. of Electrical and Electronics Engineers, Piscataway, NJ, 1993, pp. 777-781.